ISSN 1027-5495. Functional Materials, 27, No.3 (2020), p. 450-453.
doi:https://doi.org/10.15407/fm27.03.450

Photoconductivity of zinc selenide nanocrystals obtained by chemical method

***Yu.A.Nitsuk*[1], *I.V.Tepliakova*[1], *Yu.F.Vaksman*[1], *V.A.Smyntyna*[1], *I.R.Yatsunsky*[2]**

[1]Odesa I.Mechnikov National University, 2 Dvoryanskaya Str., 65082 Odesa, Ukraine
[2]Uniwersytet im. Adama Mickiewicza w Poznaniu, 1 Wieniawskiego Str., 61-712 Poznan, Poland

Received January 31, 2020

The photoconductivity spectra of ZnSe nanocrystals deposited on porous silicon wafers and wafers with silicon nanorods are studied. After deposition of ZnSe nanocrystals, a series of lines appears in the visible region of the the photoconductivity spectra of por-Si. The high-energy photoconductivity line is due to band-gap transitions in ZnSe nanoparticles. The other five lines of photoconductivity are due to transitions involving associative donor-acceptor centers, which include both intrinsic defects and uncontrolled impurity defects.

Keywords: Nanocrystals, long-wavelength photoconductivity.

Фотопровідність нанокристалів селеніду цинку, отриманих хімічним методом. *Ю.А.Ніцук, І.В.Теплякова, Ю.Ф.Ваксман, В.А.Сминтина, І.Р.Яцунський*

Досліджено спектри фотопровідності нанокристалів ZnSe, нанесених на пластинки пористого кремнію і пластинки з наностовбчиками кремнію. Після нанесення нанокристалів ZnSe у спектрах фотопровідності por-Si з'являється серія ліній у видимій області спектра. Високоенергетична лінія фотопровідності зумовлена зона-зонними переходами у наночастинках ZnSe. Решта п'ять ліній фотопровідності обумовлена переходами за участю асоціативних донорно-акцепторних центрів, до складу яких входять як власні дефекти, так і неконтрольовані домішкові дефекти.

Исследованы спектры фотопроводимости нанокристаллов ZnSe, нанесенных на пластинки пористого кремния и пластинки с наностолбиками кремния. После нанесения нанокристаллов ZnSe в спектрах фотопроводимости por-Si появляется серия линий в видимой области спектра. Высокоэнергетическая линия фотопроводимости обусловлена зона-зонными переходами в наночастицах ZnSe. Остальные пять линий фотопроводимости обусловлены переходами с участием ассоциативных донорно-акцепторных центров, в состав которых входят как собственные дефекты, так и неконтролируемые примесные дефекты.

1. Introduction

Colloidal wide-gap semiconductor nanoparticles of II–VI group are used in optoelectronics and biomedical imaging [1–8]. For example, CdSe nanocrystals are used as active media for structures emitting in the visible range [2]. Nanocomposites of CdSe/CdS, CdSe/ZnS, and CdSe/ZnSe are successfully used as photosensitive elements [9, 10]. CdSe/ZnS and CdS:Mn/ZnS nanostructures are successfully used for intravital non-toxic imaging of living cells and blood vessels [11, 12].

A new promising direction in the application of semiconductor nanoparticles is the

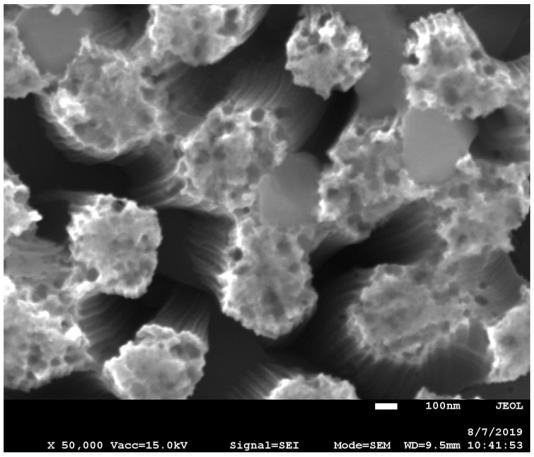

Fig. 1. SEM-image of ZnSe nanocrystals (bright structures) deposited on Si-nanopillars.

creation of solar cells based on them and increasing the efficiency of existing ones. To date, studies are known to increase the photosensitivity of titanium oxide nanorods when CdS and CdSe nanoparticles are deposited on them [13, 14]. A study of the photoconductivity of CdSe quantum dots showed their maximum photosensitivity in the region of 640 nm [15]. To expand the spectral region of photosensitivity, the use of wider-band semiconductors of this group, such as ZnSe and ZnS, is more promising. In this regard, studies of the photoconductivity of ZnSe nanocrystals are relevant.

In this work, we studied the photoconductivity of ZnSe nanocrystals deposited on conductive silicon nanorods and porous silicon. The nature of the centers responsible for the photoconductivity of ZnSe nanocrystals has been established by comparison with the optical absorption and photoluminescence spectra.

2. Experimental

Two types of nanostructured substrates were used as conductive substrates. There were plates of porous silicon (por-Si) and plates with silicon nanostubes. The procedure for their preparation is described in detail in [16].

The deposition of ZnSe nanoparticles was carried out during their growth by the colloidal synthesis method. Silicon wafers were placed at the bottom of the tube into which a 10 % aqueous solution of zinc chloride and a 10 % solution of sodium selenosulfate were added. To compare and establish the nature of the transition centers responsible for photoconductivity, control samples were applied to conductive glass. After drying,

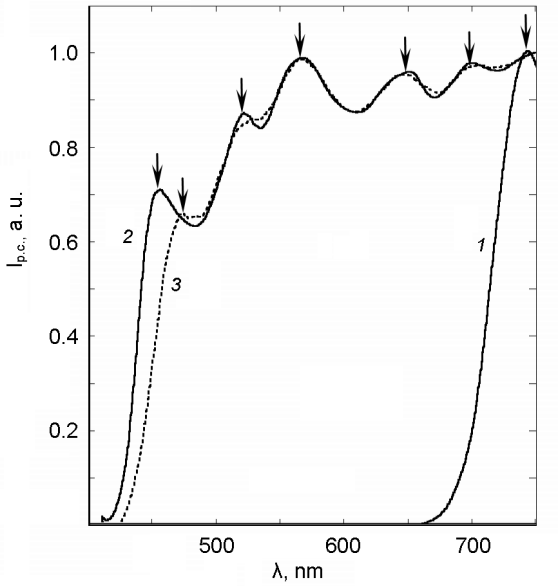

Fig. 2. Photoconductivity spectra of por-Si (*1*) and ZnSe nanocrystals (*2*, *3*). T_{meas} = 300 K (*1*, *2*) and 430 K (*3*).

the samples had a gray-yellow color. The study of X-ray diffraction showed the presence of diffraction maxima corresponding to the (111), (220) and (311) planes in ZnSe. The absence of a stabilizer in the solution promotes the growth of nanoparticles with different crystalline orientations. The SEM image of the sample deposited on porous silicon is shown in Fig. 1, where it can be seen that ZnSe nanocrystals (bright structures) are localized on the surface of Si nanorods.

The photoconductivity spectra were measured using a MUM-2 monochromator with a diffraction grating of 1200 lines/mm. The light source was a halogen lamp. The power of the luminous flux of the lamp was kept constant at different wavelengths by adjusting the incandescent current of the lamp.

In order to establish the nature of the centers responsible for photoconductivity, we measured the optical density and photoluminescence. The optical density spectra were measured using an MDR-6 monochromator with two diffraction gratings of 1200 lines/mm. An FEU-100 photomultiplier was used as a light flux recorder in the visible spectrum. Photoluminescence spectra in the visible and near infrared ranges were measured using an ISP-51 prism spectrograph. The radiation was recorded by an FEU-100 photomultiplier tube. The luminescence was excited by a solid-

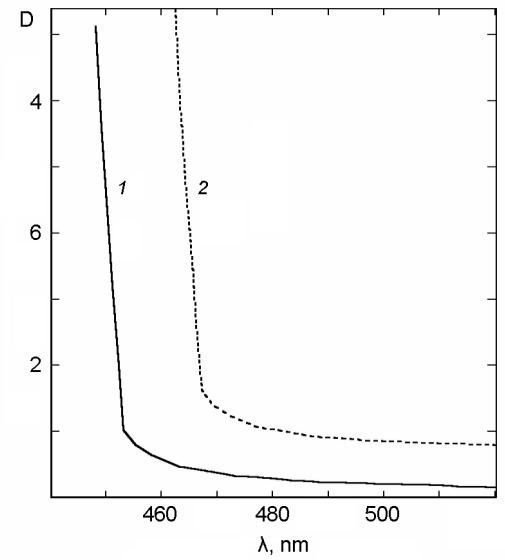

Fig. 3. Optical absorption spectra of ZnSe nanocrystals, measured at 300 K (*1*) and 430 K (*2*).

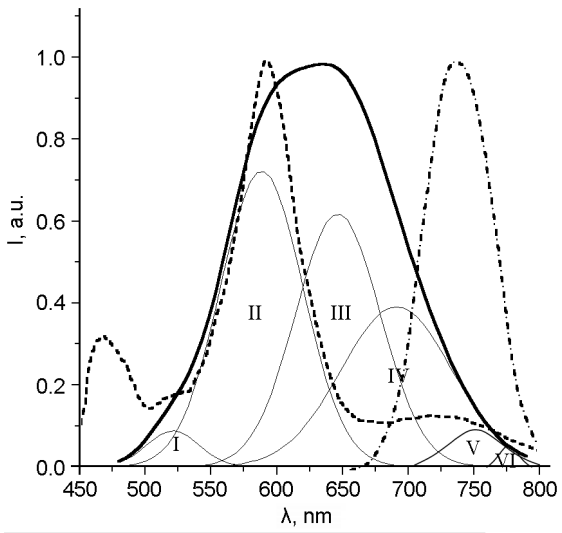

Fig. 4. Photoluminescence spectra of ZnSe/por-Si nanocrystals (dashed line), bulk ZnSe crystals (solid line) and por-Si (dash-dot line).

state laser; its quantum energy at the emission maximum was 3.1 eV.

The photoconductivity, optical absorption, and photoluminescence spectra were measured at temperatures of 300 and 430 K. For high-temperature measurements, cryostats were used, the design of which made it possible to maintain the temperature constant in the range of 77–470 K.

3.Results and discussion

A fragment of the por-Si photoconductivity spectrum in the near and infrared regions is shown in Fig. 2, curve *1*. Similar results of studies of por-Si photoconductivity were observed earlier in [17, 18]. After the deposition of ZnSe nanocrystals on the por-Si surface, a series of lines in the visible region appear in its photoconductivity spectra (Fig. 2, curve *2*). At T = 300 K, the lines are localized at 455, 520, 570, 650, and 700 nm. When the sample is heated to 430 K, the line at 455 nm is localized in the region of larger wavelengths at 472 nm. A similar shift is observed in the optical density spectra (Fig. 3). The energy corresponding to the fundamental absorption edge was determined by the extrapolation of the first linear section to the intersection with the energy axis. It coincides with the energy of photoelectric transitions corresponding to the first maximum of photoconductivity at given temperatures. Thus, it can be assumed that the first photoconductivity line is due to band-zone transitions.

The other four lines of long-wavelength photoconductivity did not shift with temperature. Moreover, their positions almost exactly coincide with the elementary emission lines of complex photoluminescence spectra of nanocrystals and bulk ZnSe crystals (Fig. 4). The elementary lines of long-wavelength emission of nanocrystals were clearly distinguished with a decrease in the concentration of zinc and selenium precursors from 10 to 2 %. In this case, the radiation intensity of nanocrystals decreased. Similar emission lines were previously observed in ZnSe single crystals by the Alentsev-Fock method [19]. The line in the region of 520 nm, which is weakly noticeable in the emission spectra, according to [20], can be due to transitions $(V_{Zn}^{-}Na_i^{+})^{*}$. The presence of sodium in nanocrystals can be explained by its presence in the precursor of selenium Na_2SeSO_3. Photoluminescence studies of CdSe nanocrystals obtained by a chemical method from sodium selenosulfate revealed the formation of sodium impurity centers in these nanocrystals [8]. The nature of the emission line at 580 nm in bulk ZnSe crystals was previously explained [19] by the presence of $(V_{Zn}^{2-}V_{Se}^{+})$-centers. The emission lines at 650, 700, and 750 nm in bulk ZnSe crystals were related [21] with associative centers ($V_{Zn}2–D_{Zn}^{-}$) with different distances between donors and acceptors, where uncontrolled Al, In, Ga impurities can act as a donor. The presence of gallium in the obtained nanocrystals was confirmed by studies of energy dispersive X-ray analysis (EDX).

Thus, the long-wavelength photoconductivity lines of ZnSe nanocrystals are due to the optical ionization of associative centers, which include both point defects of their own nature and impurity defects.

4. Conclusions

As a result of the studies, it was shown that the spectral region of the photosensitivity of porous silicon can be expanded by depositing zinc selenide nanoparticles. The nature of transitions determining the photoconductivity of ZnSe nanoparticles has been established. It was shown that the photoconductivity of zinc selenide nanoparticles is due to both band-zone transitions and transitions involving associative centers.

References

1. A.Sukhanova, A.Baranov, Y.Volkov, *Proc. SPIE*, **46**, 133 (2008).
2. A.Sukhanova, J.Devy, L.Venteo et al., *Anal. Biochem.*, **324**, 60 (2004).
3. A.E.Raevskaya, A.L.Stroyuk, S.Ya.Kuchmiy et al., *Colloid Surf.*, **290**, 304 (2006).
4. E.S.Speranskaya, N.V.Beloglazova, P.Lenain et al., *Biosens. Bioelectron.*, **53**, 225 (2014).
5. S.-H.Kang, C.K.Kumar, Z.Lee et al., *Appl. Phys. Lett.*, **93**, 191116 (2008).
6. N.N.Ledentsov, M.Grundmann, F.Heinrichsdorff et al., *IEEE J. Sel. Top. Quant.*, **6**, 439 (2000).
7. Chung Wonkeun, Yu Hong Jeong, Hee Park Sun et al., *Mater. Chem. Phys.*, **126**, 162 (2011).
8. Yu.A.Nitsuk, A.S.Leonenko, Ya.I.Lepikh, Proc, Uwbusis-2018, 8520229, 210 (2018).
9. M.A.Hines, P.Guyot Sionnest, *J. Phys. Chem.*, **100**, 468 (1996).
10. K.Rajeshwar, N.R.de Tacconi, C.R.Chenthamarakshan, *Chem. Mater.*, **13**, 2765 (2001).
11. F.Q.Chen, D.Gerion, *Nano Lett.*, **4**, 1827 (2004).
12. S.Santra, H.Yang, P.H.Holloway et al., *J. Am. Chem. Soc.*, **127**, 1656 (2005).
13. C.B.Wang, Z.F.Jiang, L.Wei, *Nano Energy*, **1**, 440 (2012).
14. L.J.Diguna, Q.Shen, J.Kobayashi et al., *Appl. Phys. Lett.*, **91**, 023116 (2007).
15. B.Pejova, A.Tanusevski, I.Grozdanov, *J. Sol. State Chem.*, **174**, 276 (2003).
16. V.A.Smyntyna, I.R.Iatsunskiy, O.V.Sviridova et al., *FIO*, **102355**, (2012).
17. O.V.Vakulenko, S.V.Kondratenko, *Semicond. Phys. Quant. Optoelectron.*, **6**, 192 (2003).
18. P.Parandiy, L.Monastyrskii, *Electron. Inform. Technol.*, **10**, 133 (2018).
19. V.V.Serdyuk, N.N.Korneva, Yu.F.Vaksman, *Phys. Stat. Sol. A*, **91**, 173(1985).
20. A.J.Rosa, B.G.Streetman, *J. Luminescence*, **10**, 211 (1975).
21. Yu.F.Vaksman, Yu.A.Nitsuk, Yu.N.Purtov et al., *Semicond.*, **35**, 920 (2001).